BROOKHAVEN NATIONAL LABORATORY

November 15, 2007 AN-624.1

Scaling fits of ppg029, ppg039 and ppg074 data

M. J. Tannenbaum*

Brookhaven National Laboratory

Upton, NY 11973-5000 USA

(Dated: November 15, 2007)

Abstract

In AN-487, ppg029 [Phys. Rev. D**74**, 072002 (2006)] and AN-562 a formula was derived for the away-side x_E distribution—for the case of a trigger particle with p_{T_t} from a hard-scattering and an associated particle with $p_{T_a} \leq p_{T_t}$—which has the nice property that it both exhibits x_E scaling and is directly sensitive to the ratio of the away jet transverse momentum, $\hat{p}_{T_a}$, to that of the trigger jet, $\hat{p}_{T_t}$, and thus to the relative energy loss of the two jets escaping from the medium in RHI collisions. Fits to the QM2006 preliminary p-p, Cu+Cu and Au+Au data were given in AN562.02 which established the validity of the formula. In this AN, I first present fits to nearly all published PHENIX p-p and d+Au two-particle correlation data. Then I review the Cu+Cu preliminary data, especially the technique of a two-component fit for finding punch-thru jets. Finally I present the fits to the ppg074 p-p and Au+Au data, which lead to several interesting conclusions on their own and in comparison to measurements by STAR.

PACS numbers: 1,1,2,3,5,8,13,21,...

*Research supported by U.S. Department of Energy, DE-AC02-98CH10886.

I. INTRODUCTION

In AN-487, ppg029 [Phys. Rev. D**74**, 072002 (2006)] and AN-562 a formula was derived for the away-side x_E distribution—for the case of a trigger particle with p_{T_t} and an associated particle with $p_{T_a} \leq p_{T_t}$—which has the nice property that it both exhibits x_E scaling and is directly sensitive to the ratio of the away jet transverse momentum, $\hat{p}_{T_a}$, to that of the trigger jet, $\hat{p}_{T_t}$, and thus to the relative energy loss of the two jets escaping from the medium in RHI collisions.

In the collinear limit, where, $p_{T_a} = x_E p_{T_t}$:

$$\left.\frac{dP_\pi}{dx_E}\right|_{p_{T_t}} \approx \langle m \rangle \, (n-1) \frac{1}{\hat{x}_h} \frac{1}{(1+\frac{x_E}{\hat{x}_h})^n} \qquad . \tag{1}$$

There are two major approximations in deriving the above equations. Incomplete Gamma functions with limits that vary with p_{T_t}, p_{T_a} and $\hat{x}_h$ are replaced by simple Gamma functions; and $\hat{x}_h$ is taken to be constant, independent of p_{T_a} for fixed p_{T_t}. The derivation assumed that the parton invariant cross section is a power law

$$\frac{d\sigma_q}{\hat{p}_{T_t} d\hat{p}_{T_t}} = \frac{A}{\hat{p}_{T_t}^n} \qquad , \tag{2}$$

and that the fragmentation function for both partons is exponential

$$D(z) = Be^{-bz} \qquad , \tag{3}$$

so that the mean multiplicity of fragments in the jet is

$$\langle m \rangle = \int_0^1 D(z) dz = \frac{B}{b}(1 - e^{-b}) \qquad , \tag{4}$$

the $\langle z \rangle$ per fragment is

$$\langle z \rangle = \frac{\int_0^1 zD(z)dz}{\int_0^1 D(z)dz} = \frac{1}{\langle m \rangle} \qquad ; \tag{5}$$

and the constraint that the fragments carry the total momentum of the gives

$$\int_0^1 zD(z)dz = \frac{B}{b^2}(1 - e^{-b}(1+b)) \equiv 1 \approx \frac{B}{b^2} \qquad , \tag{6}$$

so that

$$\langle m \rangle \approx \frac{B}{b} \approx b \qquad , \tag{7}$$

which is roughly $\langle m \rangle$=8–10 at RHIC.

The idea of symmetrizing the formula for $x_E > 1$ was discussed in AN-562 and abandoned since a better representation of the Au+Au data was found with Eq. 1 and it was felt that the region of the data with $0.2 < x_E < 0.6$ would be a good place to characterize the x_E distributions where the assumption of constant $\hat{x}_h$ as a function of x_E is not too unreasonable.

Fits to the preliminary QM06 data for $h^{\pm}$-$h^{\pm}$ data in Au+Au [J. Phys **G34**, S671–S674 (2007)] and to the π^0-$h^{\pm}$ correlations in Cu+Cu [J. Phys **G34**, S813–S816 (2007)] were given in AN-562.02 and it was concluded that the fits to Eq. 1 worked reasonably well for $p_{Tt} \geq 3$ GeV/c which established the validity of Eq. 1 for the description of (away side) x_E distributions. Thus it was time to stop fooling with preliminary data and to try to fit final published data or data submitted for publication. The data in ppg074 [arXiv:0705.3238v1] satisfy this criterion, so attention will be focussed on these Au+Au data. In this AN, I first present fits to nearly all published PHENIX p-p and d+Au data. Then I review the Cu+Cu preliminary data, especially the technique of a two-component fit for finding punch-thru jets. Finally I present the fits to the ppg074 p-p and Au+Au data. I fit the x_E distributions to the form:

$$\left.\frac{dP_\pi}{dx_E}\right|_{p_{T_t}} = N\,(n-1)\frac{1}{\hat{x}_h}\frac{1}{(1+\frac{x_E}{\hat{x}_h})^n} \qquad , \tag{8}$$

with a fixed value of $n = 8.10$ (± 0.05) which we found in ppg054 [Phys. Rev. C**76**, 034904 (2007)]. The fitted value for N is the integral of the x_E distribution which equals $\langle m \rangle$. Sometimes I also refer to Eq. 8 as $(N/\langle m \rangle)\, dP/dx_E|_{p_{T_t}}$. The two-component fit to A+A collisions uses the sum of two terms of the form of Eq. 8 with N and $\hat{x}_h$ allowed to vary in the first term, and with only N_p allowed to vary in the second term for fixed $\hat{x}_h$ given by the p-p fit.

II. FITS TO PHENIX P-P AND D+AU x_E DISTRIBUTIONS

In Fig. 1a, the π^0-$h^{\pm}$ x_E distribution from ppg029-Fig. 21 for $5.0 \leq p_{Tt} \leq 6.0$ GeV/c is shown together with the fit to Eq. 8(Eq. 1). The fit result for $\hat{x}_h = 0.69 \pm 0.03$ is comparable to but $\sim 20\%$ lower than the value of $\hat{x}_h = 0.85 \pm 0.02$ calculated in ppg029 from smearing with $\sqrt{k_T^2} = 2.68 \pm 0.07$ (stat) ± 0.34 (sys) GeV/c and shown in Fig. 1b, where the systematic errors from the uncertainty in the fragmentation function are shown as lines. The systematic

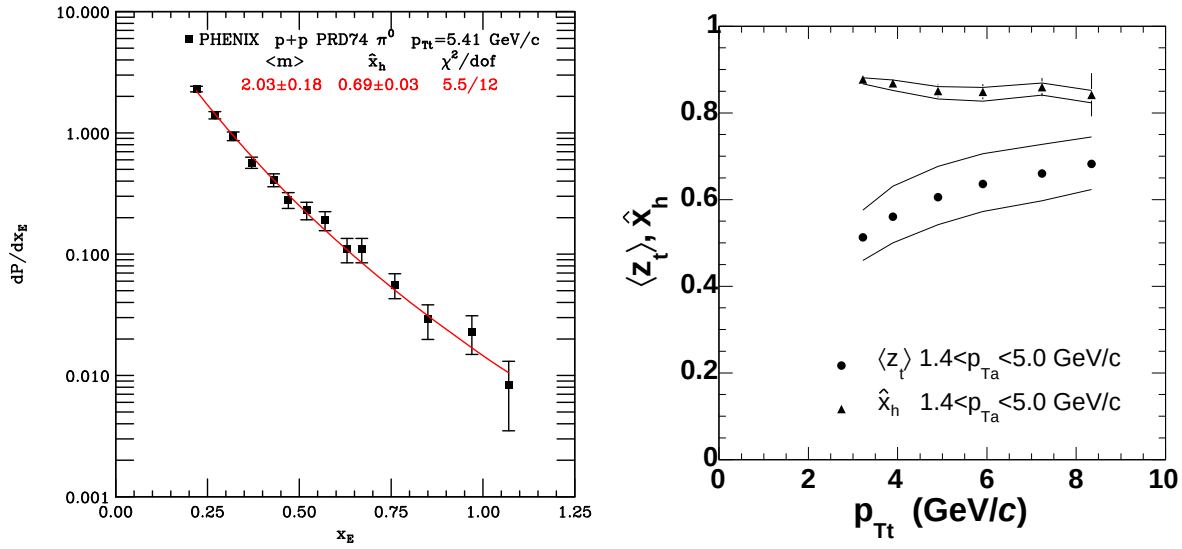

FIG. 1: a) (left) π^0-$h^\pm$ x_E distribution from ppg029 for $5.0 \leq p_{T_t} \leq 6.0$ GeV/c. Red line is fit with parameters shown. b)(right) $\hat{x}_h$ and $\langle z_t \rangle$ as a function of p_{T_t} for a wide p_{T_a} interval from calculations in ppg029.

error on $\hat{x}_h$ due to the systematic error in $\sqrt{k_T^2}$ was not discussed in ppg029, since the paper was about measuring k_T. I take the reasonable agreement of the fitted and calculated values of $\hat{x}_h$ and the splendid fit to the data in Fig. 1a as excellent in terms of characterizing the x_E distributions, but worthy of further investigation in the next study of $\pi^0 - h^\pm$ correlations in p-p collisions with much better statistics.

I liked the results of the fit for the $5.0 \leq p_{T_t} \leq 6.0$ GeV/c data in ppg029 so much that I finally got around to fitting all the data in ppg029 (Fig. 2). Notice that the fits to Eq. 8 (Fig. 2a) appear to fit the data better than the calculations in ppg029 with either the quark or gluon structure functions! The values of $\hat{x}_h(p_{T_t})$ and $N = \langle m \rangle (p_{T_t})$ from the fits in Fig. 2a are shown in Fig 3. Apart from the point at $p_{T_t} = 4.40$ GeV/c which has a terrible χ^2 due to the beyond statistical fluctuations of the data points, both $\hat{x}_h(p_{T_t})$ and $N(p_{T_t})$ tend to show a decrease with increasing p_{T_t}, with a small effect for $\hat{x}_h(p_{T_t})$ and a very large effect (2–4.5) for $N(p_{T_t})$. Notice that the largest value of N comes from the data with the highest value of x_E for the first data point, thus requiring the largest extrapolation to zero.

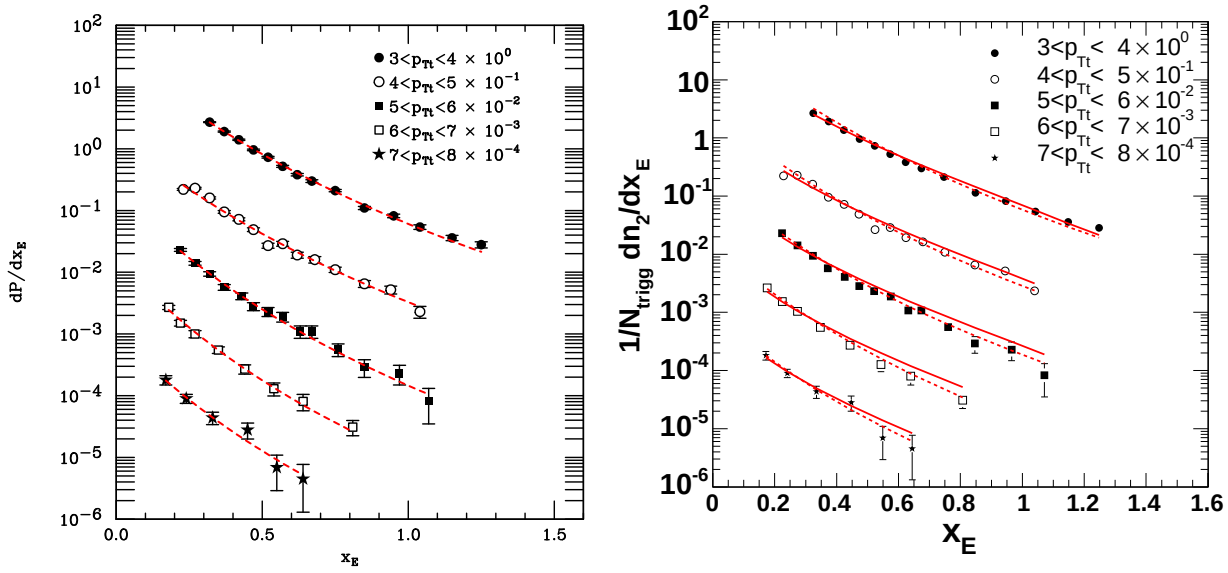

FIG. 2: a) (left) π^0-$h^\pm$ x_E distributions from ppg029. Red lines are fits to Eq. 8. b)(right) Fig. 21 from ppg029 with calculations from quark (solid) and gluon (dashed) fragmentation functions.

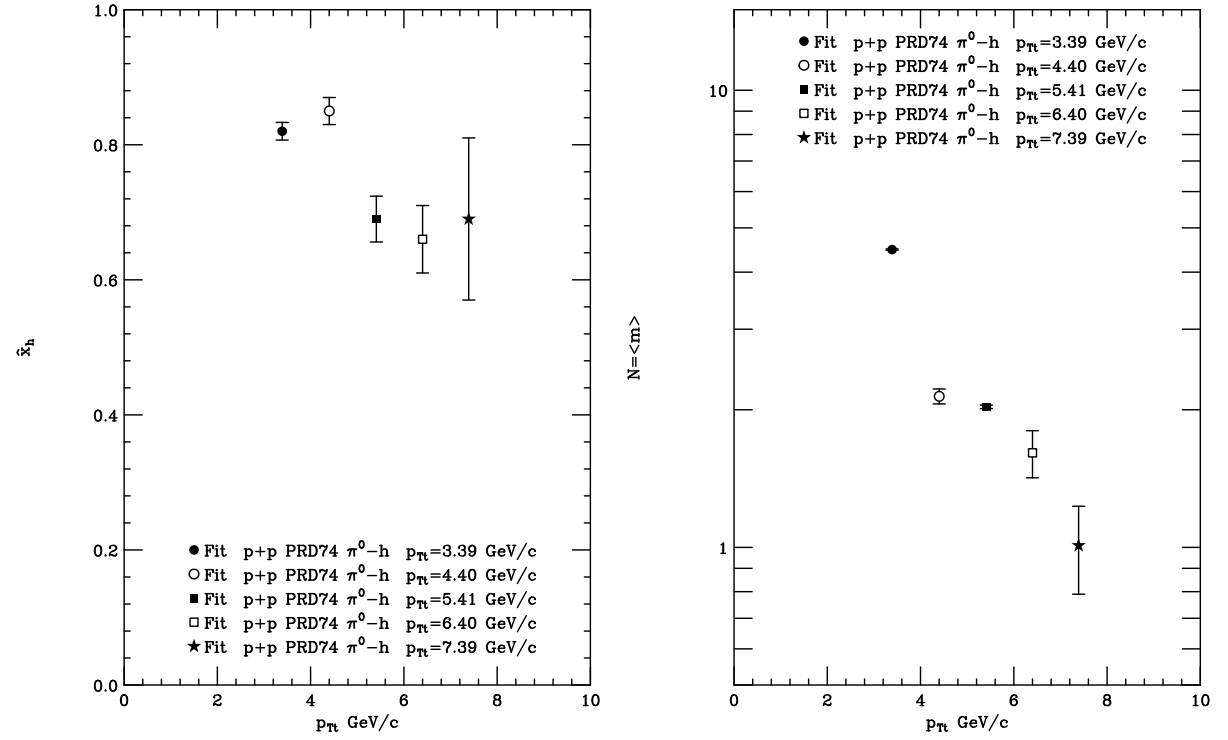

FIG. 3: a) (left) Values of $\hat{x}_h(p_{T_t})$ from fits in Fig. 2a; b) (right) Values of $N = \langle m \rangle\,(p_{T_t})$.

Interestingly, fits to $\pi^0 - h^{\pm}$ and $\pi^{\pm} - h$ correlations in ppg039 (Figs. 4–6) give values for $\hat{x}_h$ in p-p collisions closer results of the values of $\hat{x}_h \gtrsim 0.80$ in the ppg029 calculation than the fits to the ppg029 data (Fig. 3a). The d+Au fits also suggest a systematic trend of lower $\hat{x}_h$ with increasing p_{T_t} (Fig. 6b), but the errors are too large to claim anything significant. One thing is clear from Figs. 4–6, fits to all the published PHENIX x_E distributions in p-p and d+Au are quite good, with values for the fitted $\hat{x}_h$ in excellent agreement with each other (Fig. 6b). Newer data, with better statistics, will allow us to make more detailed studies of the p_{T_t}, particle type and other dependences.

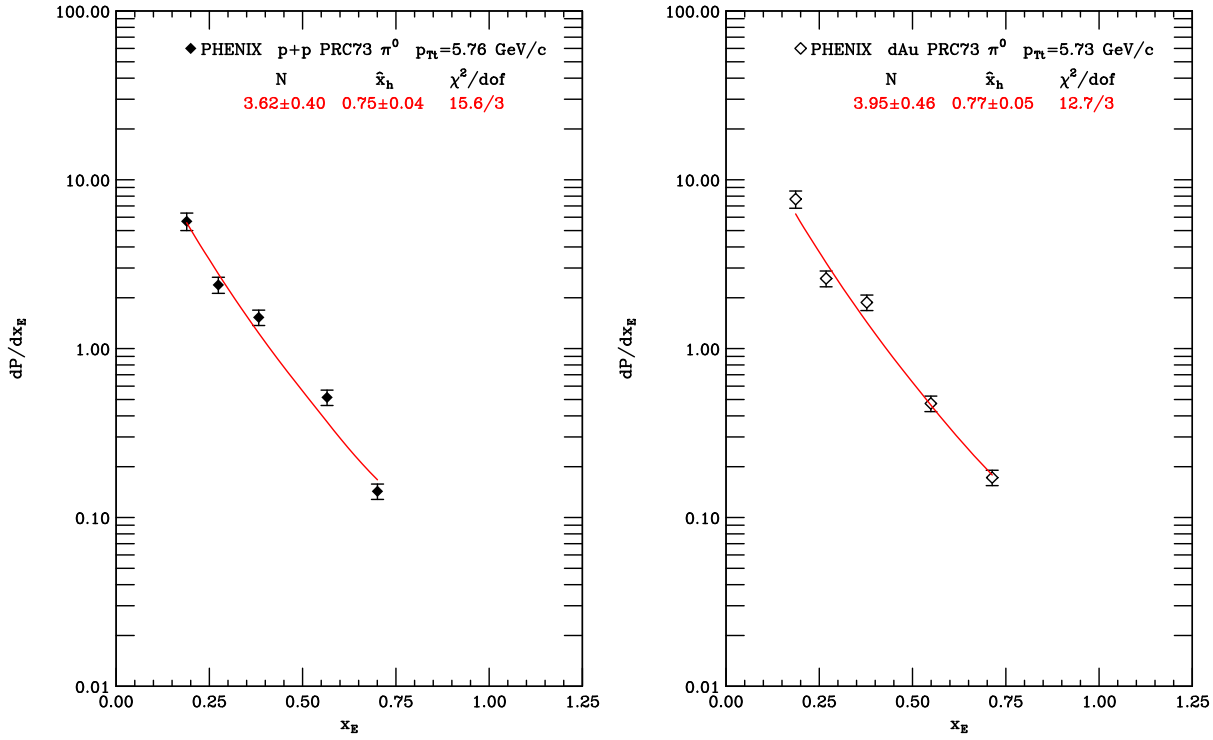

FIG. 4: $\pi^0 - h$ data from ppg039 and fit: a) (left) p-p, b) (right) d+Au

In Fig. 7a, I have plotted all the PHENIX d+Au x_E distributions on a single plot in the spirit of ppg039-Fig. 30 together with the fit for $5 \leq p_{T_t} \leq 6$ GeV/c and Magestro's d+Au data from STAR [PRL97, 162301 (2006)] for $8 \leq p_{T_t} \leq 15$ GeV/c. I have previously commented in AN562.02, as shown in Fig. 7b, that the STAR Au+Au distribution is too flat compared to other distributions in the same p_{T_t} range and Fig. 7a clearly shows this effect in d+Au. This raises several questions, e.g. why does the PHENIX data stop at $x_E \sim 0.8$? is the STAR 'flatness' at larger values of x_E (p_{T_a}) due to degrading momentum resolution? etc. I also noticed that the STAR PRL 97 data is actually flatter than the STAR Au+Au data

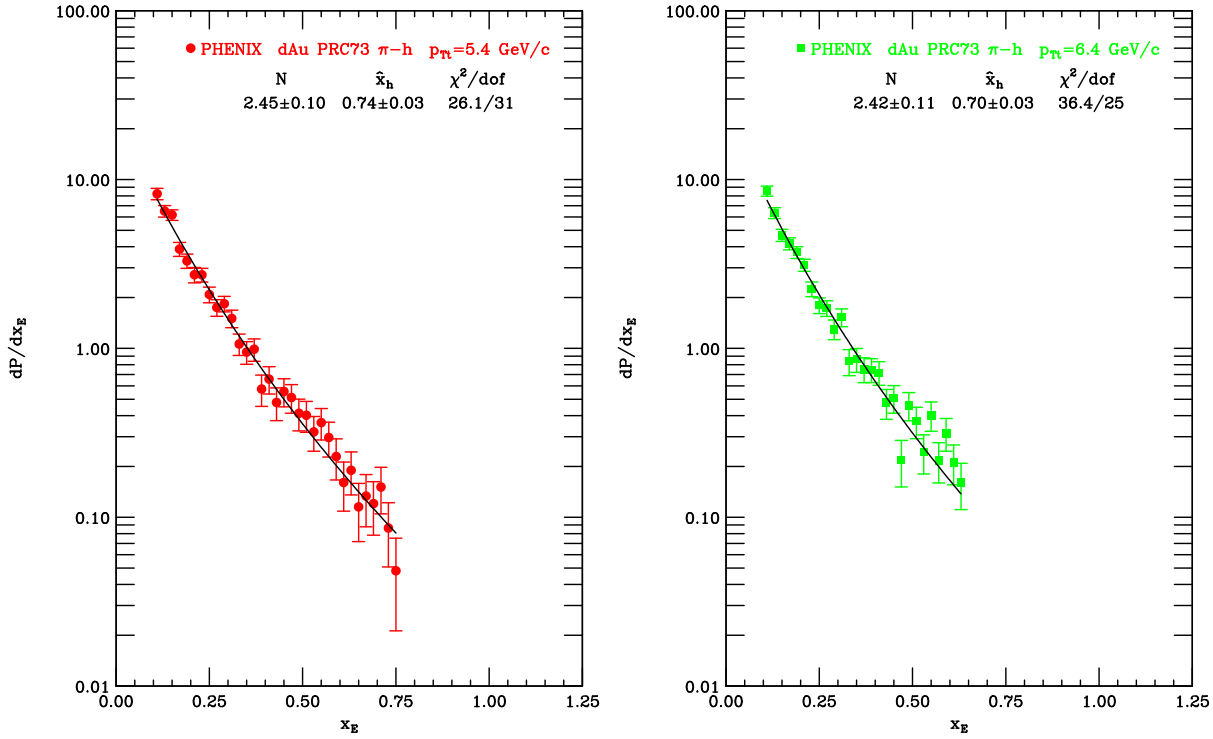

FIG. 5: a) (left) d+Au $\pi - h$ data and fit for $p_{Tt} = 5.4$ GeV/c. b) (right) $p_{Tt} = 6.4$ GeV/c.

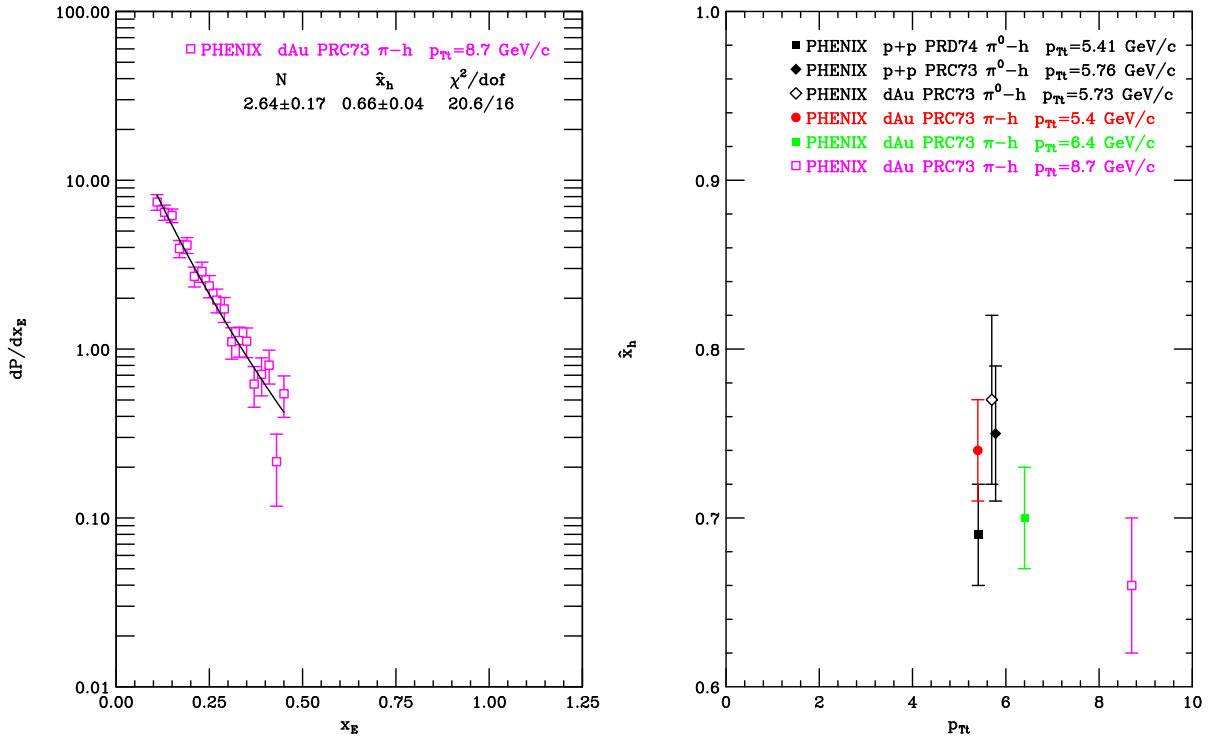

FIG. 6: a) (left) $\pi - h$ $p_{Tt} = 8.7$ GeV/c. b) (right) $\hat{x}_h$ from fits.

from Phys. Rev. Lett. **95**, 152301 (2005) (see Fig. 7b) which I first showed at Hard Probes 2006 and then discussed in a few conference proceedings [e.g. see PoS(CFRNC2006)001]. On the other hand, when I normalized STAR's x_E distributions in PRL 97 to agree with PRL 95 in the region of overlap, there appeared to be a sharp break at $x_E \gtrsim 0.4$ suggestive of a two-component distribution. This idea stuck with me as described in the next section.

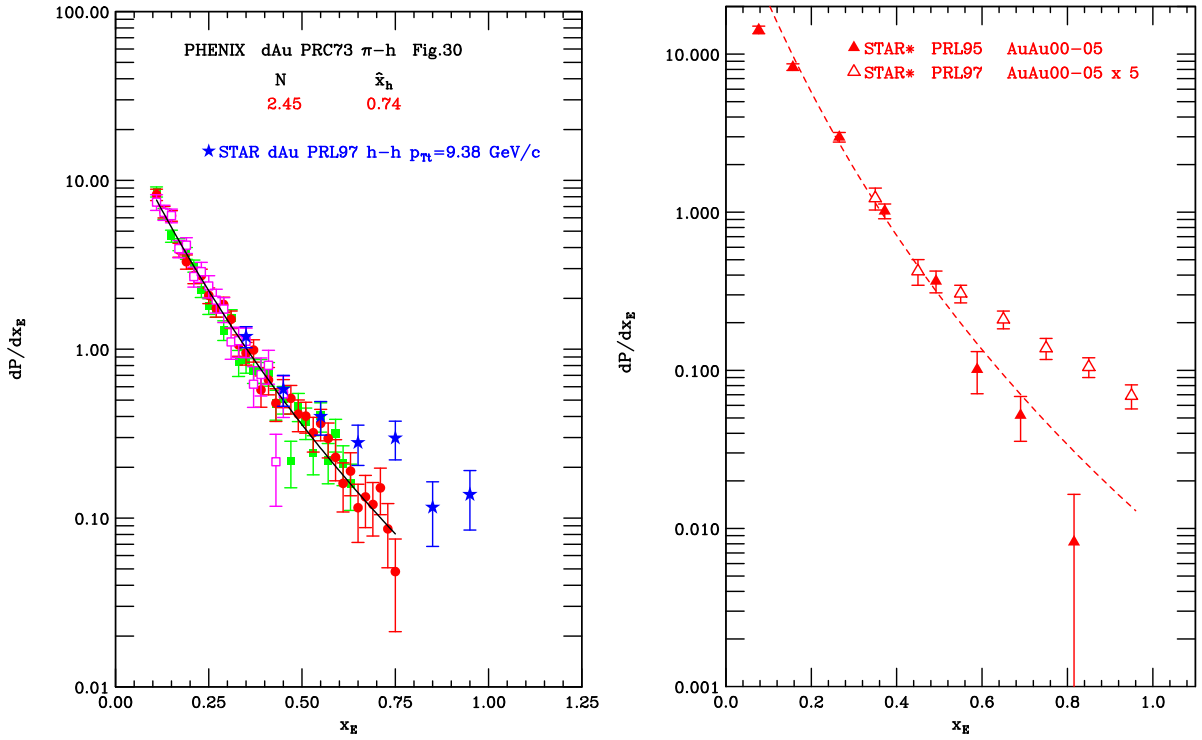

FIG. 7: a) (left) PHENIX d+Au distributions from Figs. 5 and 6 together with STAR d+Au data from PRL 97. b) (right) STAR $h^{\pm} - h^{\pm}$ x_E distributions in Au+Au central collisions. Solid triangles with $p_{T_t} \approx 4.6$ GeV/c from Phys. Rev. Lett. **95**, 152301 (2005); dashed line is eyeball distribution with $\hat{x}_h = 0.48$. Open triangles are from Phys. Rev. Lett. **97**, 162301 (2006) with $p_{T_t} \approx 9.4$ GeV/c, arbitrarily normalized by me so that the lowest two points lie on the $p_{T_t} \approx 4.6$ GeV/c data.

III. FITS TO THE CU+CU PRELIMINARY DATA AND THE ISSUE OF PUNCH-THRU JETS.

One aspect of the Cu+Cu preliminary data from AN-562.02 is worth reviewing here. Fits of Eq. 8 to the $\pi^0 - h$ correlations for the Cu+Cu preliminary data analysis for QM2006

are shown in Fig. 8a for p-p and Fig. 8b for Cu+Cu for $5.0 \leq p_{T_t} \leq 10.0$ GeV/c. The p-p spectra appeared too flat to me in AN562.02 as shown explicitly by the fitted value of $\hat{x}_h = 0.90 \pm 0.01$ in stark disagreement with all the PHENIX published values (Fig. 6b). Also the data for $x_E > 0.75$ is definitely flatter than the curve leading to the relatively poor $\chi^2/\mathrm{dof} = 71/15$. I deleted the lowest point from the fit because it contributed nearly 200 to the χ^2 by itself. The fit including this lowest point, shown by the black dashed line in Fig 8a, deviates even more from the points at $x_E > 0.75$. The Cu+Cu central data (Fig 8b) show this same flattening of the distribution for $x_E > 0.75$ as indicated by comparison to the standard fit to Eq. 8 (dashed line), which has a decent $\chi^2/\mathrm{dof} = 58/16$ (in comparison to the p-p fit) but falls well below the data points at larger x_E. This gave me the idea that flat part of the spectrum at large $x_E \gtrsim 0.75$ might represent a punch-thru peak, in which case $I_{AA}^{\mathrm{punchthru}}(x_E)$ would be constant and equal to the fraction of the events in the CuCu data that punched through.

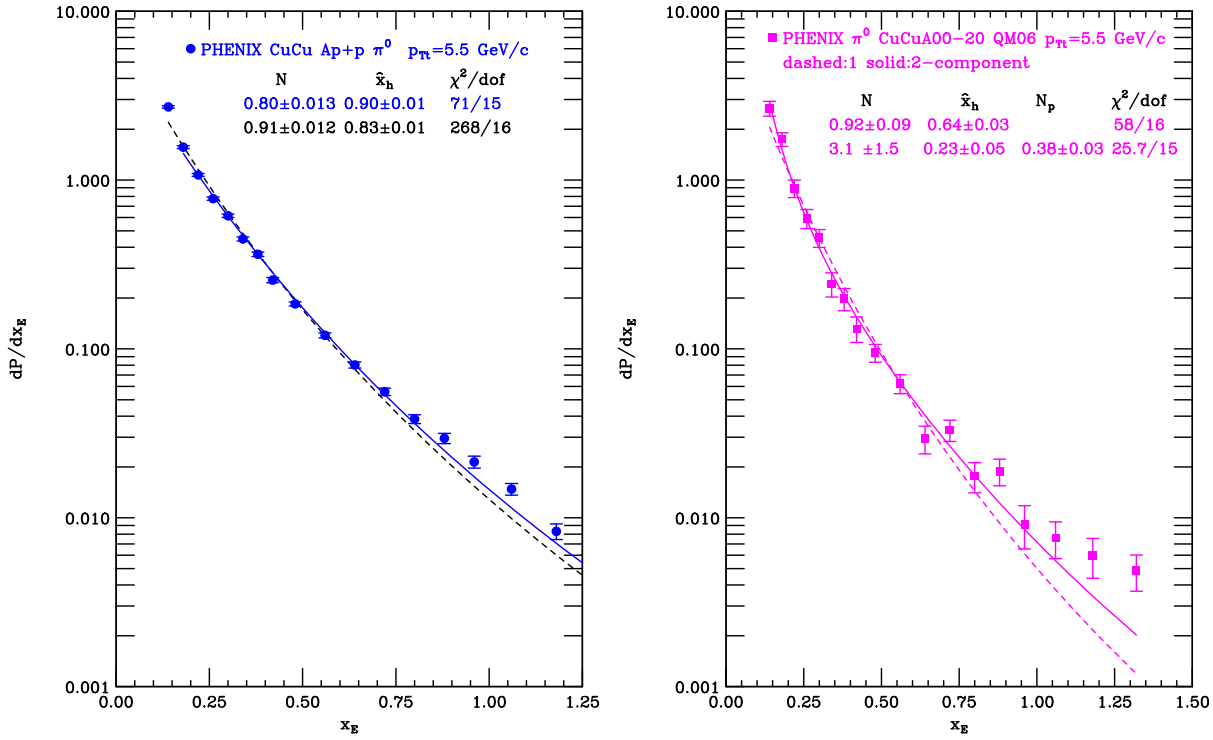

FIG. 8: a) (left) π^0-$h^\pm$ x_E p-p comparison plot for CuCu data. The solid blue line and values in blue are a fit do the data excluding the point at $x_E = 0.140$; the black dashed fit and black values include all points (with much worse χ^2). b)(right) π^0-$h^\pm$ x_E distribution for CuCu0020 with single component (dashes) and punchthru (solid) fits.

Thus, I decided to fit the Cu+Cu distributions to a two-component distribution, with one component allowing N and $\hat{x}_h$ to vary and the other component with $\hat{x}_h$ fixed to the value from the p-p fit but with its own normalization, N_p. The value of $I_{AA}(x_E)$ for the punch-thru, i.e the fraction of the triggers that punched through, is then N_p divided by $N = 0.80$ from the fit to the p-p data Fig 8a. The two component fit is shown by the solid line on Fig. 8b and is much closer to the data with a much improved $\chi^2/\mathrm{dof} = 25.7/15$, just at the edge of a 90% confidence interval (1-pvalue $\sim 5\%$). Additionally, the likelihood ratio test, the $\Delta\chi^2$ for 1 dof which is at the significance of $\Delta\chi^2 > 30/1$ (off the charts, much smaller probability than 0.001 that this happens at random). If the 2-component fit is to be believed in reality, as the statistical significance indicates, it says that there is one component in which the away-jet in Cu+Cu central (Fig. 8b) has a fraction 0.23/0.90=26% of the momentum of the away jet in p-p collisions and a punch-thru component (with the same $\hat{x}_h$ as in p-p collisions) with a fraction, $I_{AA} = 0.38/0.80 = 0.48$, of the triggers, so half and half energy-loss and punch-thru. This result is sufficiently suggestive and interesting that it bears examining with the final data.

IV. PPG074

In this section, the PHENIX final p-p and Au+Au central data of ppg074 [arXiv:0705.3238] submitted for publication are fit using Eq. 1. In ppg074, the properties of possible punch-through jets and the medium reaction were characterized by dividing the correlation function into 2 regions a head region H, where the jet correlations appear in p-p collisions, and a shoulder region S where our famous mach cone or medium reaction appears (Fig. 9).

The x_E distributions in the head region, which I will call HO for Head-Only, and the head + shoulder region $H + S$ were obtained for both p-p and Au+Au data; but rather than trying to scale one distribution onto the other in ppg074, the distributions for Au+Au and p-p were divided by each other (following, in my opinion a bad precedent from STAR, except for punch-thru correlations as noted above, and same-side correlations which are said to be surface biased with minimal or no energy loss, in which case $I_{AA}(p_{T_t}) \approx 1$) to obtain

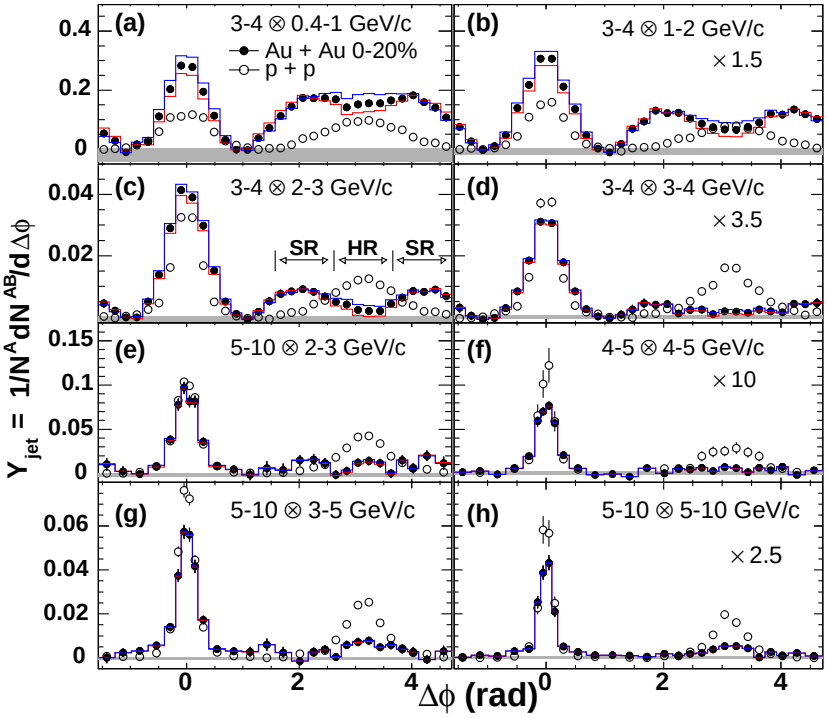

FIG. 9: ppg074-Fig. 1.

the variable:

$$I_{AA} = \frac{dP_\pi^{AA}/dx_E|_{p_{T_t}}}{dP_\pi^{pp}/dx_E|_{p_{T_t}}} = \frac{dP_\pi^{AA}/dp_{T_a}|_{p_{T_t}}}{dP_\pi^{pp}/dp_{T_a}|_{p_{T_t}}} \quad , \tag{9}$$

where to keep the reader's attention p_{T_t} and p_{T_a} in this AN are referred to as p_T^A and p_T^B in ppg074. The distributions (Fig. 10a) show the standard effect that they are larger than 1 for lower x_E and smaller than 1 at larger x_E, which screams out to me (but apparently to few others) that this is exactly what I expect from an $x_E/\hat{x}_h$ distribution when the away jet loses energy relative to the trigger jet in an AuAu collision. A feature that my skeptical nature appreciates about Fig. 10a is that the full jet distribution $H+S$ is compared to HO because the region of the $H+S$ distribution is such that $\int d\phi \cos 2\phi \sim 0$ so that any issues of how the v_2 of the background is subtracted are moot. The conclusion in ppg074 from Fig. 10a was that for the two higher p_{T_t} values, I_{AA} becomes constant at a level of 0.2–0.3, the same as R_{AA} (for π^0, not $h^\pm$), which one must admit is a bit hard to confirm from the scale of the figure. In my way of thinking, a constant I_{AA} implies a punchthrough jet which has not lost any energy, i.e. has the same x_E distribution as in p-p collisions. I call this the two component model and will attempt to see whether I can observe this effect below by fitting

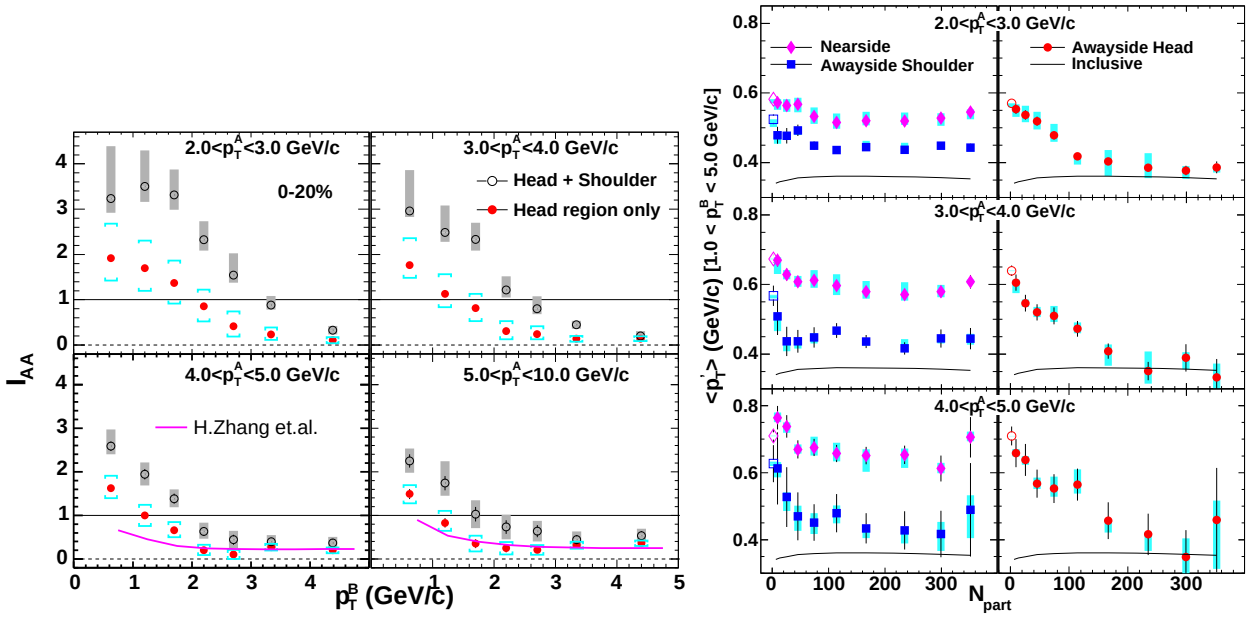

FIG. 10: a) (left) I_{AA} distributions (ppg074-Fig.3) for HO and $H+S$ for Au+Au central. b) (right). Truncated $\left\langle p_T^{'} \right\rangle$ (ppg074-Fig. 4)

the individual x_E distributions for Au+Au and p-p. In my opinion, the most interesting conclusion from ppg074, shown in Fig. 10b is that the dependence of the shape of the H and S p_{T_a} distributions as a function of centrality, as represented by the truncated $\langle p_{T_a} \rangle$, are different: the S distribution has constant $\langle p_{T_a} \rangle$ above 50 participants while the $\langle p_{T_a} \rangle$ of the H steadily decreases with increasing centrality (showing increasing energy loss) reaching equality to the S (around 10% lower) for $N_{\rm part} > 200$. The constancy of S with centrality is taken to be a reflection of an intrinsic property of the response of the medium to the energetic jets, although why the properties of the medium (Temperature, density, volume, ...) and the effects thereof would not depend on centrality remains a mystery (to me).

A. Scaling fits to the x_E distributions

I decided to put my money (at least my effort) where my mouth is and try to analyze the x_E distributions that make up Fig. 10a by fitting to Eq. 8. The results of these fits compared to the measurements are shown in Figs. 11–14 with summaries of the fit parameters in Figs. 15–17. The fits are acceptable for all the p-p data for both $H+S$ and HO. However

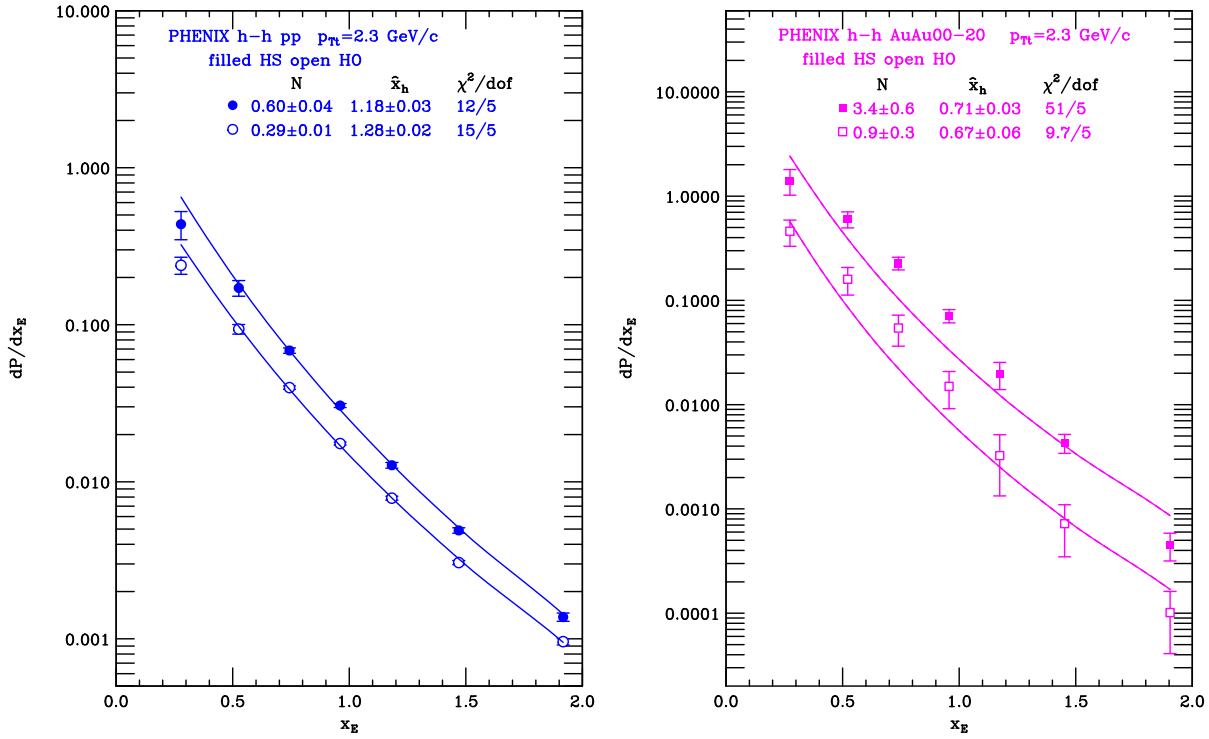

FIG. 11: a) (left) p-p $H+S$, HO data and fit. b) (right) same for AuAu00-20%.

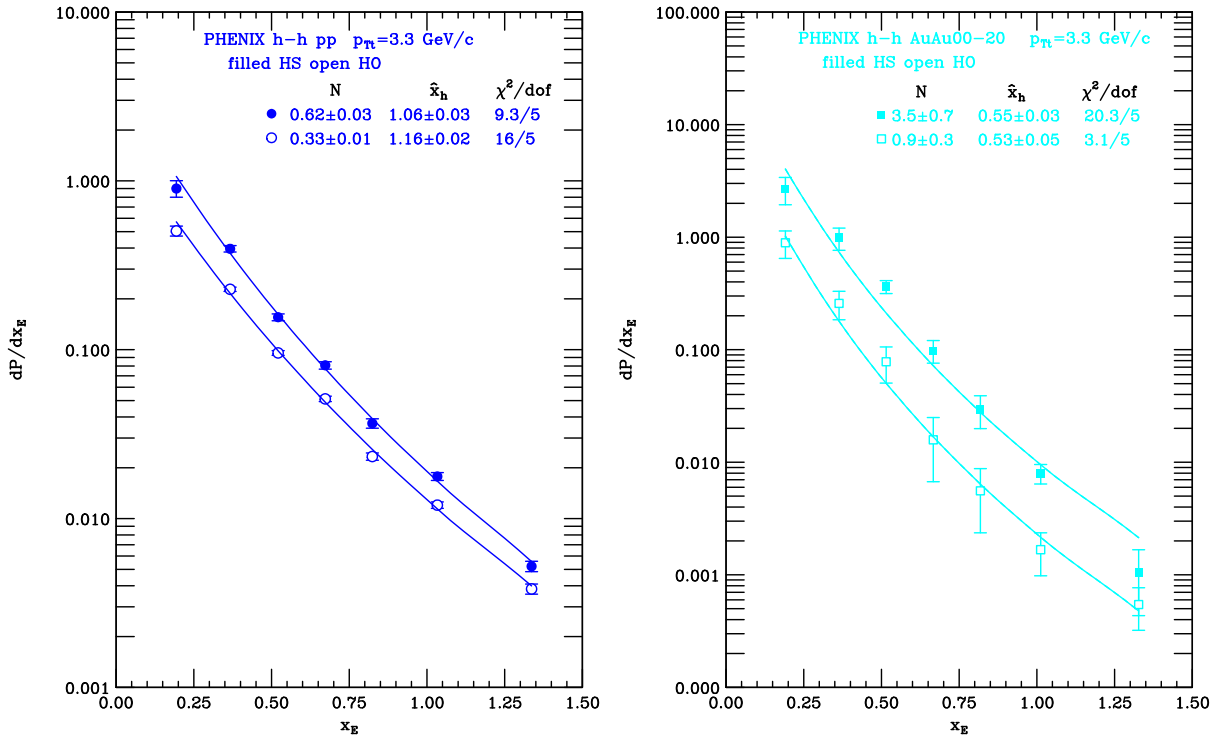

FIG. 12: a) (left) p-p $H+S$, HO data and fit. b) (right) same for AuAu00-20%.

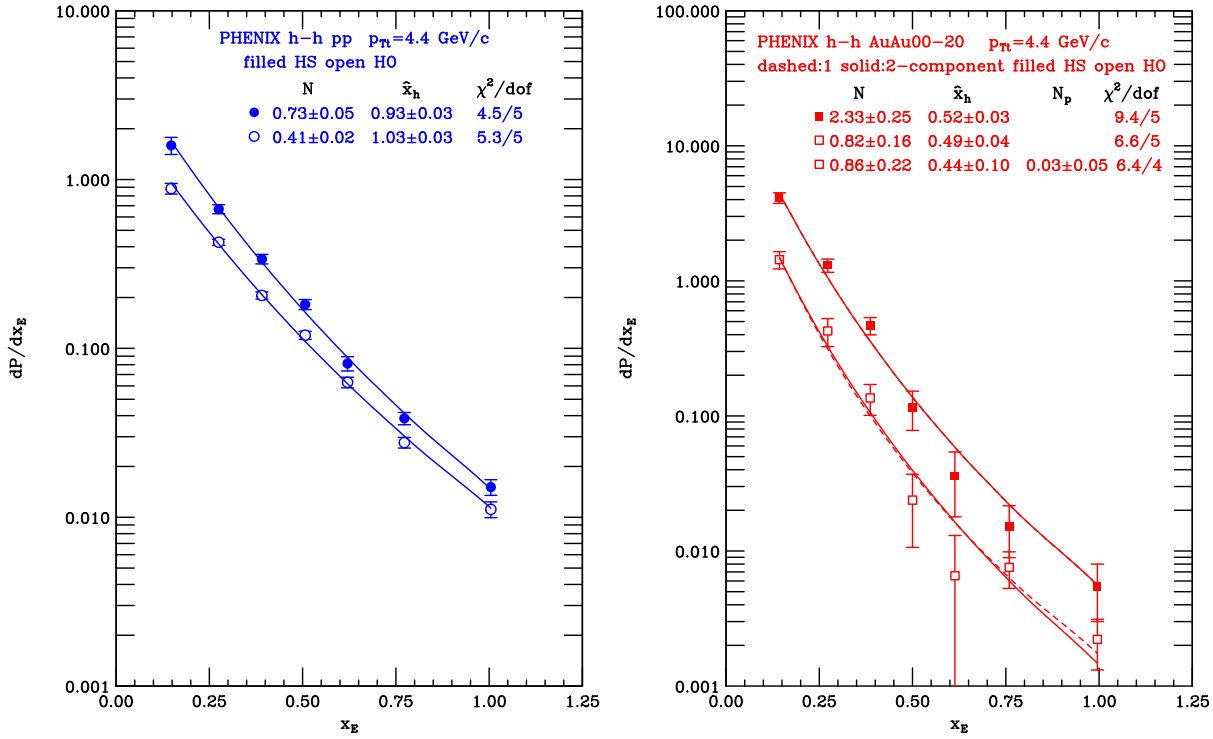

FIG. 13: a) (left) p-p $H+S$, HO data and fit. b) (right) same for AuAu00-20%.

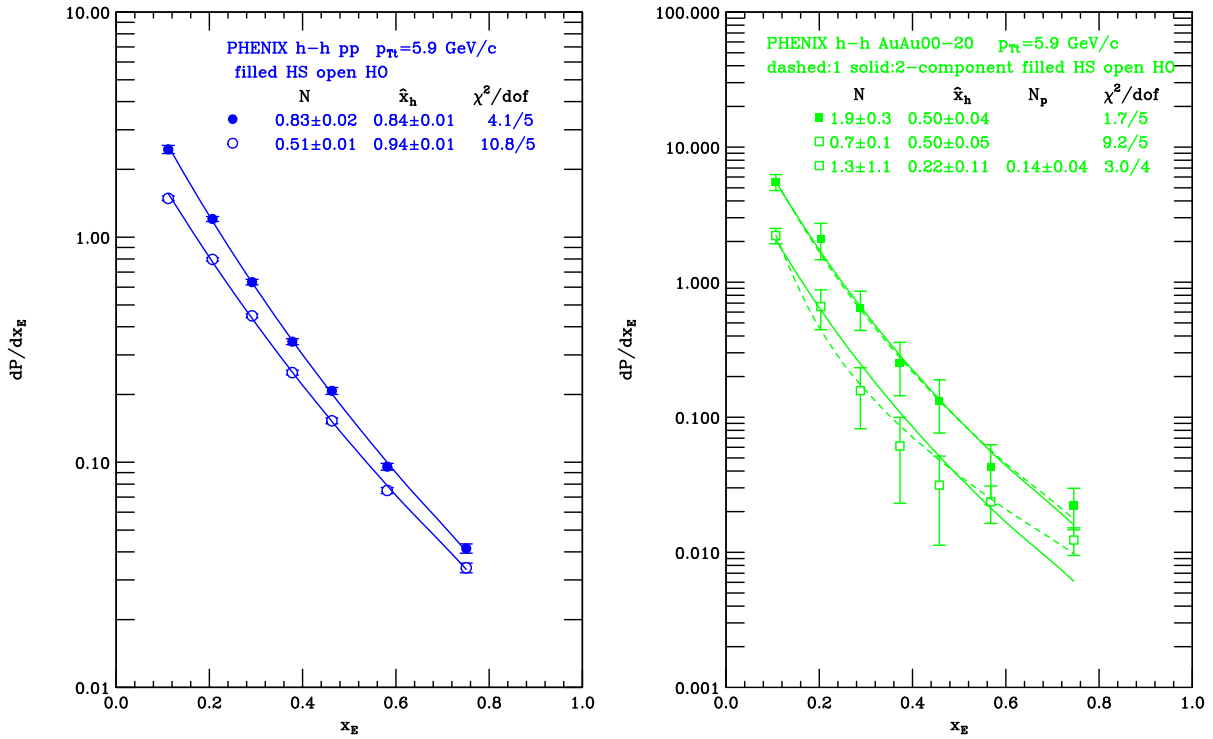

FIG. 14: a) (left) p-p $H+S$, HO data and fit. b) (right) same for AuAu00-20%.

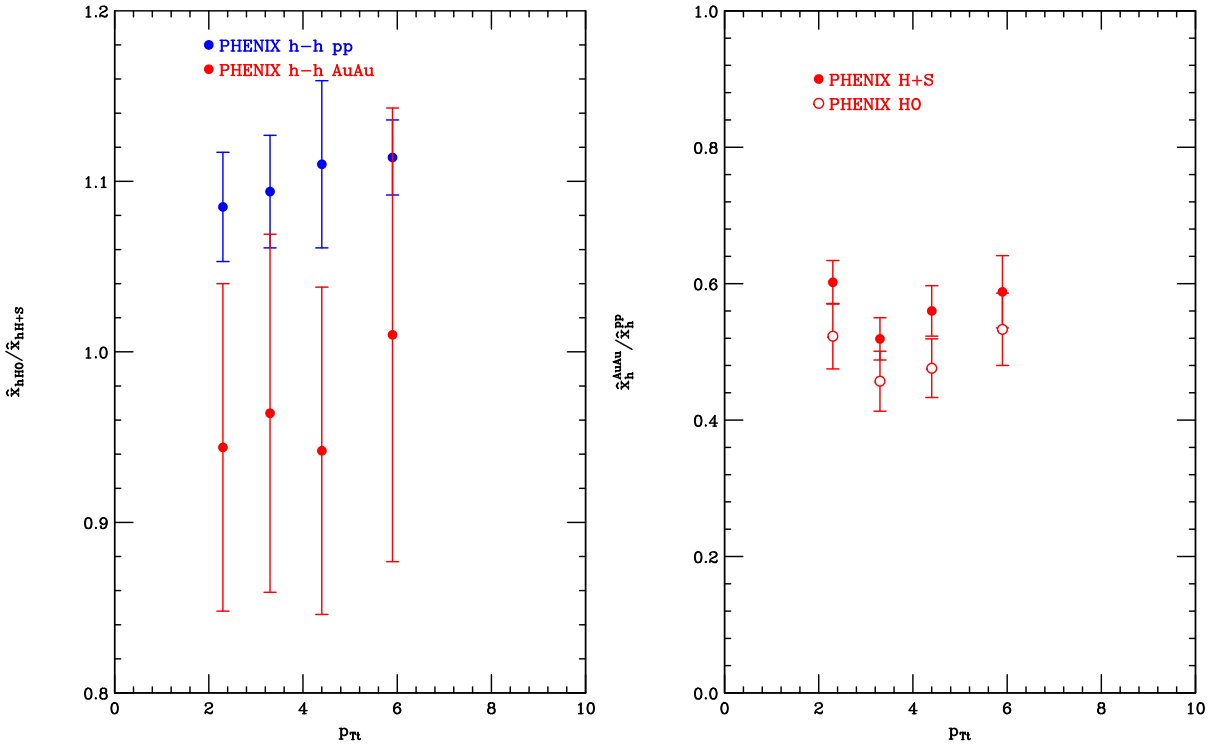

FIG. 15: a) (left) Ratio of $\hat{x}_h$ for HO to $H+S$. b) (right) ratio for Au+Au to p-p.

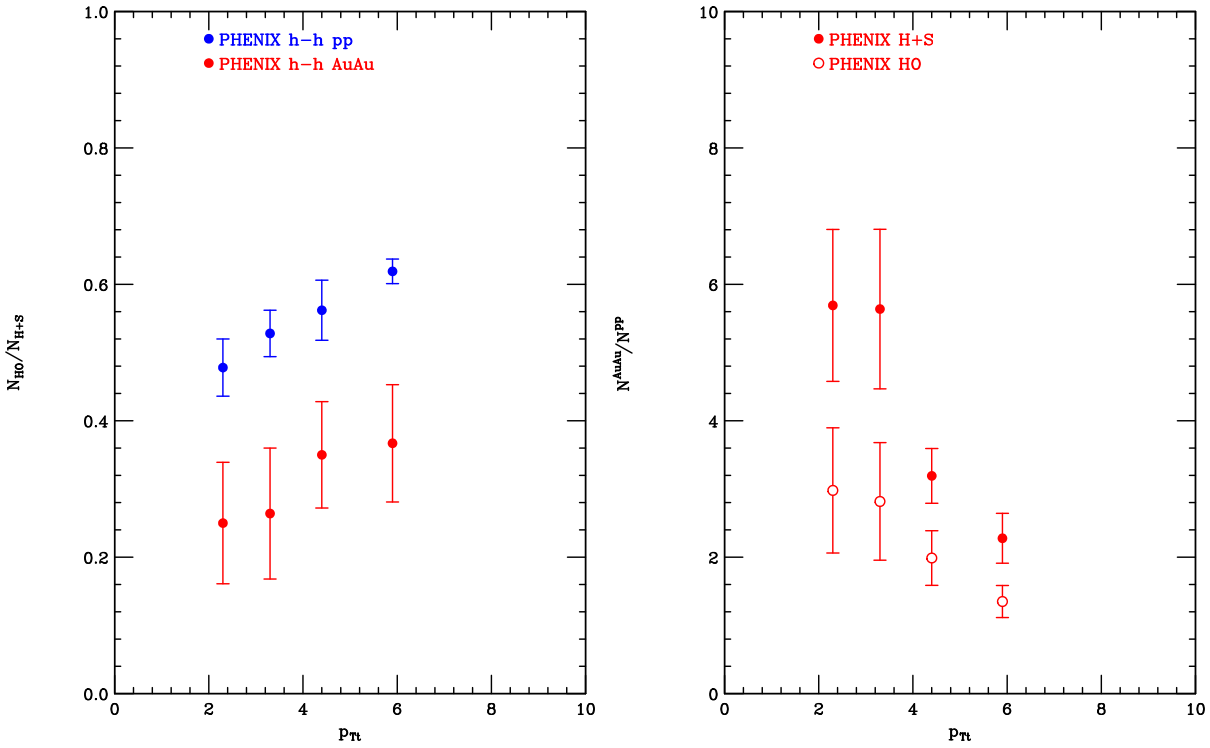

FIG. 16: a) (left) Ratio of $N = \langle m \rangle$ for HO to $H+S$. b) (right) ratio for Au+Au to p-p.

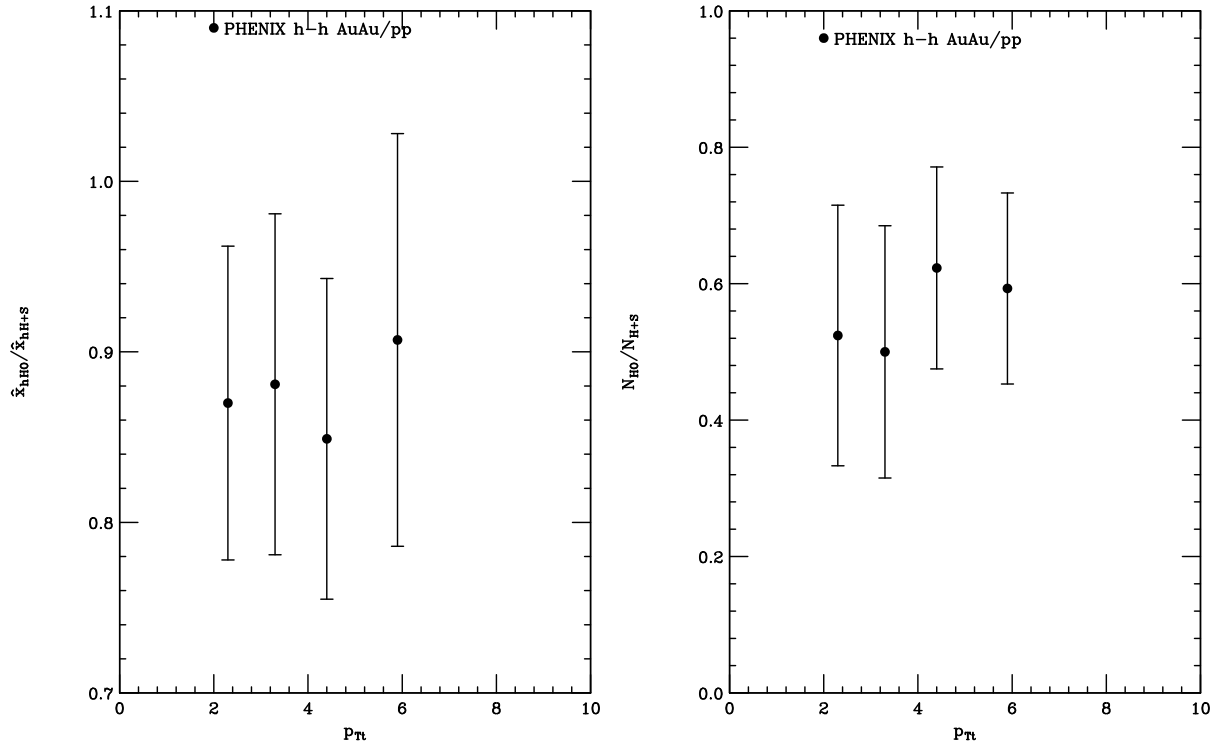

FIG. 17: Double ratio of fit parameters for HO to $H+S$ in Au+Au relative to p-p. a) (left) $\hat{x}_h$; b) (right) $N = \langle m \rangle$.

the N values are all a factor of $\sim 2-3$ larger for ppg074 than for ppg029, ppg039; but Jiangyong tells me that a $\Delta\eta$ correction, a factor of 2 on the away side, was not made in ppg074 which likely explains the difference. So long as the $\Delta\eta$ correction is also not made to the Au+Au data in ppg074, then the Au+Au/p-p ratios should be valid. A direct comparison of the p-p data and fit of Fig. 1a to Fig. 14a is shown in Fig. 18, so a factor of 2 upward shift of the ppg074 data would solve most of the discrepancy and the larger $\hat{x}_h$ could be attributed to the fact that ppg079 is $h-h$ rather than π^0-h. For completeness, I must point out that the ppg074 data were not given as x_E distributions but as p_{T_a} distributions for a range of p_{T_t}. I transformed the distributions to x_E distributions by using $\langle p_{T_t} \rangle$ for the range assuming an invariant $p_{T_t}^{-8.1}$ cross section, e.g. for $5 < p_{T_a} < 10$ GeV/c, I calculated $\langle p_{T_t} \rangle = 5.9$ GeV/c for calculating x_E.

The quality of the fits to the Au+Au data is acceptable and comparable to the quality of the p-p fits except for the lowest $p_{T_t} = 2.3$ GeV/c Au+Au data (Fig. 11b) where the $H+S$ fit has $\chi^2/\text{dof} = 51/5$ which is not acceptable. However the fit does follow the trend of the

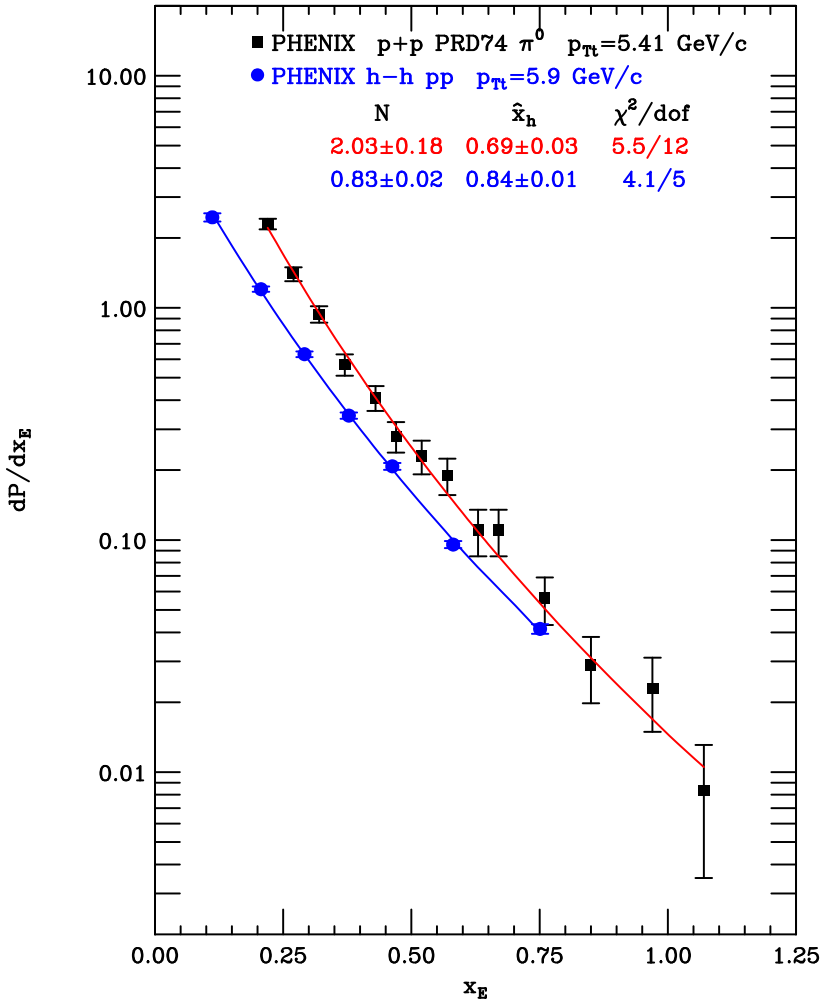

FIG. 18: x_E distribution and fits for $\pi^0 - h$ in p-p collisions from ppg029 compared to that for $h - h$ from ppg074 at roughly the same p_{T_t}.

data very nicely, so I keep it. For the lowest two p_{T_t} bins, 2.3 and 3.3 GeV/c I tried fits for both the p-p and Au+Au data leaving out the point at lowest x_E (Figs. 19, 20, black lines and legend). These fits have much better χ^2/dof but have a different trend at the lowest x_E than the data, so I don't use them. This might be a lesson that sometimes fits with poor χ^2/dof can be more useful for understanding the data than fits with better χ^2.

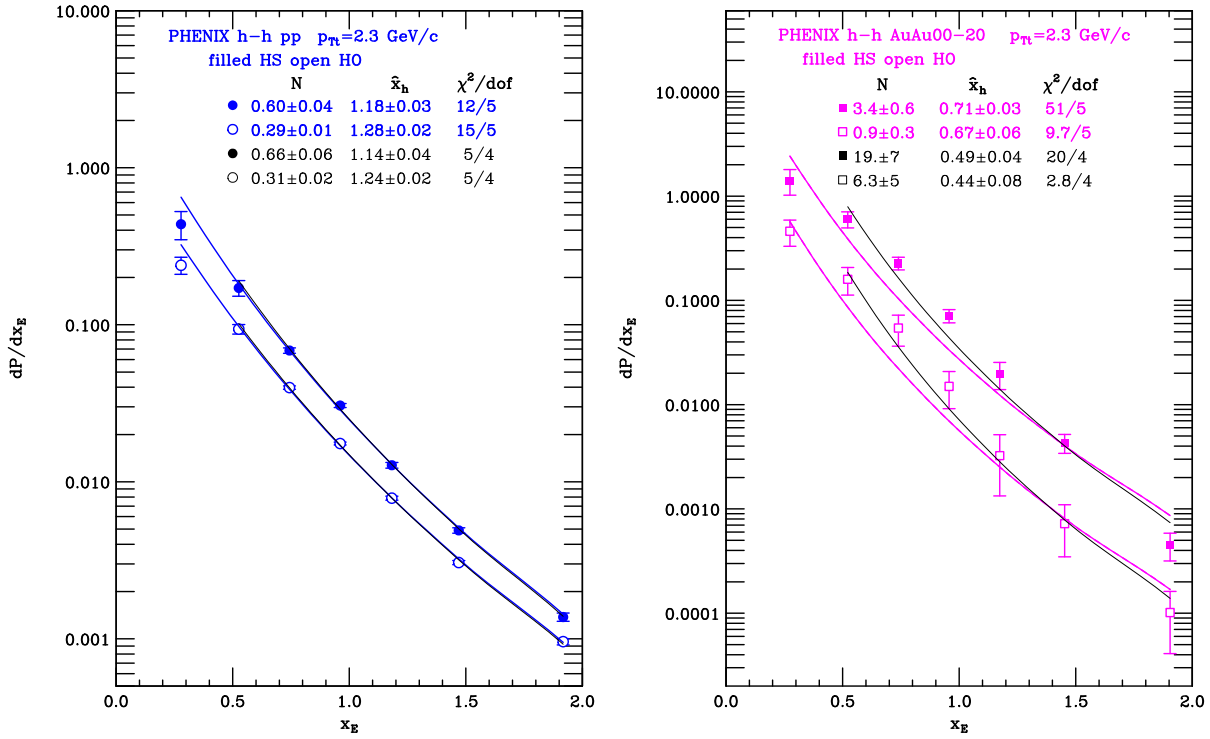

FIG. 19: Same as Fig. 11 except black lines and legend represent fits without point at lowest x_E.

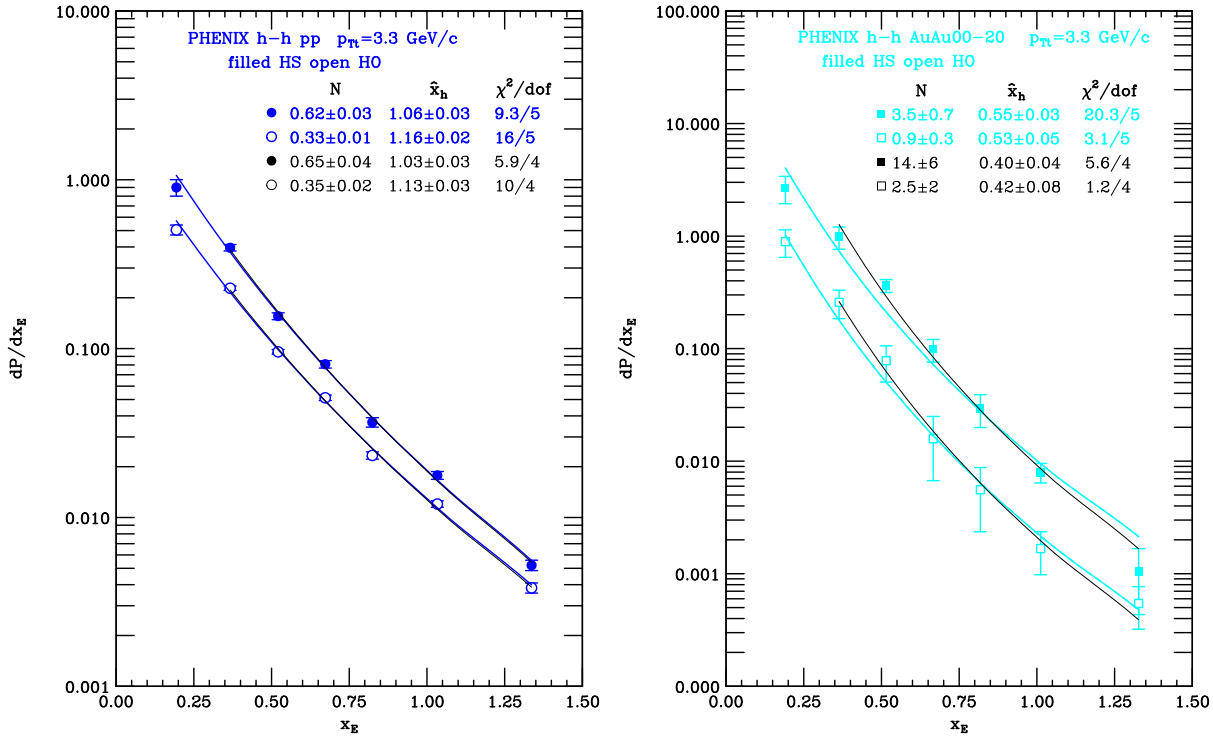

FIG. 20: Same as Fig. 12 except black lines and legend represent fits without point at lowest x_E.

B. What did I learn?

My summary of the parameters from the fits of Eq. 8 to the p-p and Au+Au x_E distributions for the HO and $H+S$ regions is shown in Figs. 15–17. The shape of the $H+S$ and HO distributions has a constant ratio of $\hat{x}_{hHO}/\hat{x}_{hH+S}$ as a function of p_{T_t} in both p-p and Au+Au (Fig. 15a). The HO distributions are $\sim 10\%$ flatter than $H+S$ in p-p collisions and $\sim 5\%$ steeper in Au+Au. The suppression, the ratio of the energy of the away jet to that of the trigger jet in Au+Au relative to p-p (Fig. 15b), indicates a large relative energy loss $\hat{x}_h^{\rm AuAu}/\hat{x}_h^{\rm pp} \sim 0.55$ for both HO and $H+S$ independent of p_{T_t} and again $\sim 10\%$ smaller for HO than $H+S$.

The values of N, the integral of the distribution, the mean multiplicity of the jet, show similar a similar trend. The ratio of N_{HO}/N_{H+S}, which is the fraction of the $H+S$ peak that is in the head region, is roughly independent of p_{T_t} for p-p and Au+Au (Fig. 16a), although the p-p data might suggest an increasing trend with p_{T_t}—implying a narrowing of the clear p-p peak—and about 50% smaller in Au+Au than in p-p for all p_{T_t}. This, together with the fact that the double ratio of the parameters in the $HO/H+S$ regions in Au+Au/p-p (Fig. 17) is a constant, independent of p_{T_t} for both $\hat{x}_h$ and N suggests to me that the head is just a small slice of the same stuff as the $H+S$ in both p-p and Au+Au central collisions, i.e. there is really no difference in the properties of the H and S regions. Perhaps this means that there is really no actual head in central Au+Au collisions from a punch-thru jet. On this point, the good news is that only one Au+Au plot shows evidence of punch-thru. The highest p_{T_t} data for Au+Au (Fig. 14b) clearly shows the effect of punch-thru for the HO region but not for the $H+S$ by the likelihood-ratio test of the two-component fit (dashed lines) to the standard fit (solid lines). Only for the HO region does the addition of a second component with the $\hat{x}_h$ of the p-p data improve the χ^2 by a statistically significant amount, $\Delta\chi^2 = 6.2/1$ or less than 2% chance that this is a random effect of constraining one parameter. This is also shown by the fitted parameter $N_p = 0.14 \pm 0.04$ being > 3 standard deviations from 0, and also by the point with the largest x_E being much higher than the solid curve, but right on the dashed curve.

C. Something else interesting

I didn't discuss the ratio of the jet fragment multiplicities in Au+Au/p-p, N^{AuAu}/N^{pp} (Fig. 16b). For both the HO and $H+S$ regions the multiplicity, $N = \langle m \rangle$, the integral of the x_E distribution, is increased by a factor of 2–3 for $H+S$ in the highest two p_{T_t} bins and a factor $\sim 40\%$ less for HO. The $H+S$ increase seems much larger for the lowest two p_{T_t} bins but this probably stems from the fits being well above the trend of the data in the extrapolation to low x_E (e.g. Fig. 11b). This result is the first clear indication to me that the famous $I_{AA}(x_E)$ plots which are all greater than 1 for smaller x_E and less than 1 for larger x_E require more than a simple scaling of the x_E distribution from p-p to Au+Au due to the larger energy loss of the away-jet relative to the surface biased trigger jet. At first, I didn't pay any attention to this feature of the ppg074 data which I don't think is derivable from the I_{AA} distributions in Fig. 10 without also knowing either the p-p or Au+Au x_E distributions and being able to perform the integral over the invisible lower x_E range (using the Eq. 8) as done in this AN. However, John Chen and Justin Frantz, in the Sept 27, 2007 hard-photon PWG, claimed by a different method that the energy rather than the mean multiplicity carried by the trigger and away jets increases relative to the trigger p_{T_t} in Au+Au compared to p-p collisions.

In my opinion, an increase in energy is much harder to understand than an increase in $\langle m \rangle$ due to both a shift in the spectrum and a pile-up at low x_E. The $\langle m \rangle$ can increase if e.g.: i) the away quark jet radiates a gluon, reducing its energy, which results in a shifted x_E spectrum i.e. $\hat{x}_h \ll 1$ when it fragments; ii) the radiated gluon, of energy $\gtrsim$1 GeV, also fragments to soft particles resulting in a second source of $\langle m \rangle$ concentrated at low x_E, roughly doubling the total $\langle m \rangle$. Of course, I don't have a clue why Eq. 1 is smart enough to take this two-parton fragmentation into account. It is difficult to understand how the energy could increase in Au+Au compared to p-p since we know from ppg054 that the entire shift in the spectrum to cause $R_{AA} = 0.2$ is less than 16–18% leaving very little available energy to add to the trigger p_{T_t}. On the other hand, we later found out that the large increase in the same side energy did not include the trigger p_{T_t}, so it represents only a slight decrease of the trigger $\langle z_t \rangle$ from 0.83 to 0.77 which is not so huge. Nevertheless, these observations, probably the first integrals of the energy and multiplicity in jet correlations in Au+Au collisions, lead

our thinking and possibly our knowledge in new and interesting directions.

It was pointed out, after further reflection, that both these effects, the increase in away-side integrated multiplicity $\langle m \rangle$ by a factor of 2–3 from p-p to Au+Au central and the increase of the both the same and away side $\sum_i |p_{Ti}|$, for fixed p_{T_t}, in Au+Au central compared to p-p collisions were previously reported in one of STAR's best papers by Fuqiang Wang [Phys. Rev. Lett. **95**, 152301 (2005)].

V. CONCLUSIONS

Essentially all the published or submitted PHENIX p-p and A+A x_E distributions give reasonably good fits to Eq. 8. This provides a quantitative basis to evaluate the expected parton energy loss in the medium via LPM bremsstrahlung by characterizing all the measured x_E distributions by two parameters, $N = \langle m \rangle$, the mean multiplicity of fragments from the away jet, and $\hat{x}_h = \hat{p}_{T_a}/\hat{p}_{T_t}$ the ratio of the transverse momenta of the away jet to that of the trigger jet. In ppg074, the medium effect on the away jet was characterized by the truncated mean p_{T_a}. However, since the present method gives a valid statistical description of the full x_E distribution, which is not exponential, while the truncated mean merely samples a local slope in a fixed region of p_{T_a}, which varies in x_E with different p_{T_t}, variations of the truncated mean may just represent variations of the region of x_E sampled rather than changes in any property of the medium (e.g. see Fig. 19 in ppg029 [Phys. Rev. D**74**, 072002 (2006)]). I have tried to demonstrate here that using Eq. 8 to characterize the away x_E distribution gives reasonable fits and quantitative information about the away-side yield and the energy loss of the away-jet relative to the trigger jet which is superior to admiring plots of I_{AA} and perhaps is less biased than simply measuring the truncated mean. (I think that it also works for the same side distribution, but I'll leave that to somebody else.) I do hope that this AN leads to a more general adoption of this fit method in PHENIX.

One final issue concerns punch-through jets for which there are clear statistical indications in Fig. 14b for HO in Au+Au-central and Fig. 8b for Cu+Cu-central. You may wonder why I harp on this. As I noted previously in Fig. 7b, there appeared to be a sharp break in the STAR PRL97 data with respect to the PRL95 data when I normalized them to each other in the region of overlap. I then suggested to STAR that they should measure a few more

low x_E points for the higher p_{T_t} trigger. I don't know if they actually listened to me but at QM2006 Mark Horner [J. Phys **G34**, S995 (2007)] showed improved x_E (what they call z_T) distributions where a two-component distribution is evident for $6 < p_{T_t} < 10$ GeV/c (Fig. 21a), with a clear break in slope for $z_T \geq 0.5$. I don't understand why STAR doesn't make a bigger deal about these observations, which still gives us a chance. I think that the two-component punch-thru scenario is much more reasonable in the LPM formalism than the single component punch-thru favored by STAR in PRL 97. If the away-jet doesn't radiate a coherent LPM $\sim 1-2$ GeV gluon, then it punches-through with essentially the same $\hat{x}_h$ as in p-p collisions. If it does radiate then the spectrum is scaled by the lower energy of the away parton which radiated relative to the trigger parton leading to a lower $\hat{x}_h$ in Au+Au than in p-p collisions.

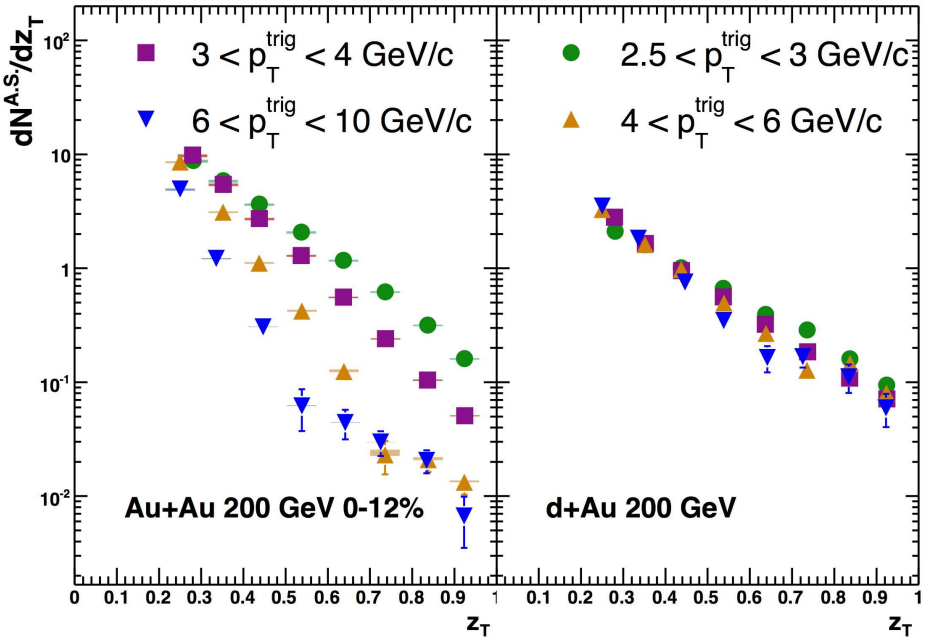

FIG. 21: Away-side $x_E = z_T$ distributions for various p_{T_t} from Horner-QM2006-[J. Phys **G34**, S995 (2007)] for a) (left) Au+Au central, b) (rignt) d+Au.

While staring at Fig. 21, it appeared to me that the slopes of the Au+Au data steepen with increasing p_{T_t} (Fig. 21a) much more than the d+Au data (Fig. 21b) whereas our data show a constant ratio of slopes ($\hat{x}_h$) in Au+Au/p-p with increasing p_{T_t} in the same range (Fig. 15b). Is this a disagreement? Amazingly, when I replotted our Au+Au and p-p data for the $H + S$ to look like Fig. 21 (see Fig. 22 which I hadn't made until writing this), the

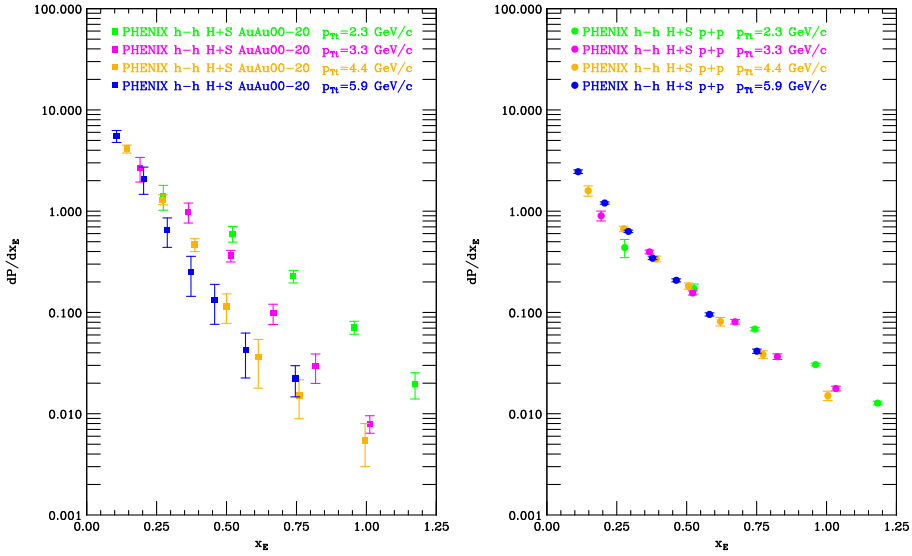

FIG. 22: PHENIX Away-side x_E distributions for various p_{T_t} for a) (left) Au+Au central, b) (rignt) p+p.

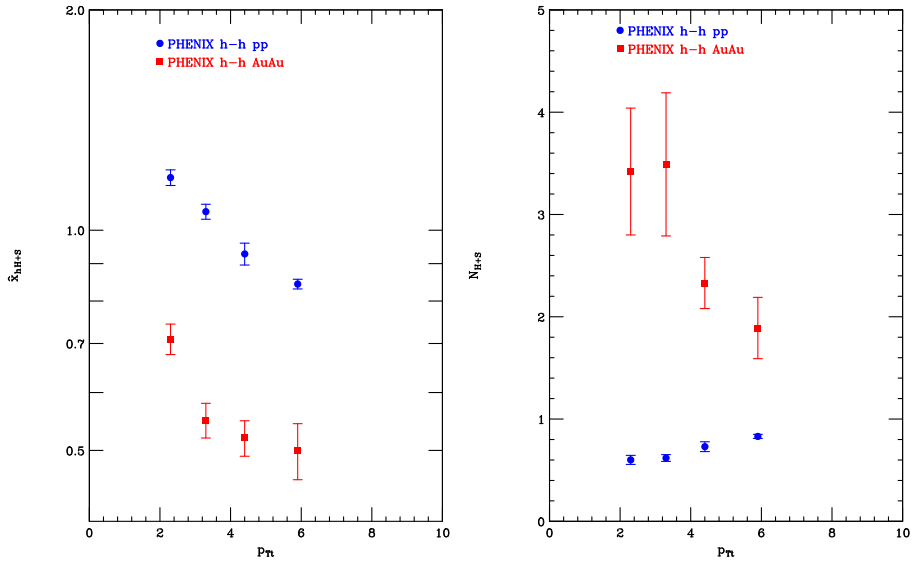

FIG. 23: a) (left) $\hat{x}_h$ for $H+S$ in pp and Au+Au 00-20%. b) (right) $N = \langle m \rangle$ for $H+S$ in p-p and Au+Au 00-20%.

plots look much the same and in fact a plot of $\hat{x}_h$ and $N = \langle m \rangle$ for our $H+S$ data shows a clear systematic reduction of $\hat{x}_h$ with increasing p_{T_t} in p-p collisions (Fig. 23a). Although the effect isn't convincing for Au+Au, the ratios of the $\hat{x}_h(p_{T_t})$ in Au+Au to p-p are consistent with being constant as shown more clearly in Fig. 15b.

It seems clear to me that if one stares at the data long enough trends become evident. I

also think that we may be able to sort out all these issues with our own data first, if we hop to it, because, for some reason, STAR seems to be on the slow side in interpreting their own data.

xE fits April13,2007. I fit to N*(n-1)/[xh(1+xE/xh)^n				h-h							
Data	Deck	N		xh		n		Nn		ch sq/dof	
ppg074.fit	hsfitxE2007-2p-nots										
HO/ H+S ratio pp		**0.478**	**0.042**	**1.085**	**0.032**						
1-pp H+S2.3notsym	**hsfitxE2007-1nots**	**0.601**	**0.044**	**1.18**	**0.029**	**8.1**	**fixed**			**11.8/5**	**2.36**
m1= lowest point deleted		0.662	0.06	1.14	0.03	8.1	fixed			4.7/4	1.18
HO/ H+S ratio AuAu		**0.250**	**0.089**	**0.944**	**0.096**						
2-AuAu0020H+S 2.3		**3.42**	**0.62**	**0.71**	**0.034**	**8.1**	**fixed**			**50.7/5**	**10.14**
m1		19.4	7	0.49	0.04	8.1	fixed			20/4	5.00
Suppression		**5.691**	**1.113**	**0.602**	**0.032**						
3-pp HO 2.3		**0.287**	**0.014**	**1.28**	**0.02**	**8.1**	**fixed**			**15/5**	**3.00**
m1		0.31	0.02	1.24	0.02	8.1	fixed			5/4	1.25
4-AuAu0020 HO 2.3		**0.855**	**0.26**	**0.67**	**0.06**	**8.1**	**fixed**			**9.7/5**	**1.94**
m1		6.33	4.9	0.44	0.08	8.1	fixed			2.8/4	0.70
Suppression		**2.979**	**0.918**	**0.523**	**0.048**						
HO/ H+S ratio pp		**0.528**	**0.034**	**1.094**	**0.033**						
5-pp H+S 3.3		**0.619**	**0.033**	**1.06**	**0.025**	**8.1**	**fixed**			**9.25/5**	**1.85**
m1		0.65	0.04	1.03	0.03	8.1	fixed			5.9/4	1.48
HO/ H+S ratio AuAu		**0.264**	**0.096**	**0.964**	**0.105**						
6-AuAu0020H+S 3.3		**3.49**	**0.7**	**0.55**	**0.03**	**8.1**	**fixed**			**20.3/5**	**4.06**
m1		13.8	6	0.396	0.042	8.1	fixed			5.6/4	1.40
Suppression		**5.638**	**1.170**	**0.519**	**0.031**						
7-pp HO 3.3		**0.327**	**0.012**	**1.16**	**0.022**	**8.1**	**fixed**			**15.8/5**	**3.16**
m1		0.346	0.015	1.13	0.025	8.1	fixed			10.3/4	2.58
8-AuAu0020 HO 3.3		**0.921**	**0.28**	**0.53**	**0.05**	**8.1**	**fixed**			**3.1/5**	**0.62**
m1		2.5	1.8	0.42	0.08	8.1	fixed			1.2/4	0.28
		4.9	9.4	0.33	0.19	8.1	fixed	0.02	0.03	0.9/3	0.08
Suppression		**2.817**	**0.862**	**0.457**	**0.044**						
HO/ H+S ratio pp		**0.562**	**0.044**	**1.110**	**0.049**						
9-pp H+S 4.4		**0.73**	**0.048**	**0.928**	**0.032**	**8.1**	**fixed**			**4.54/5**	**0.91**
HO/ H+S ratio AuAu		**0.350**	**0.078**	**0.942**	**0.096**						
10-AuAu0020H+S 4.4		**2.33**	**0.25**	**0.52**	**0.029**	**8.1**	**fixed**			**9.36/5**	**1.87**
		2.33	0.25	0.52	0.029	8.1	fixed	0	0.07	9.36/4	2.34
Suppression		**3.192**	**0.402**	**0.560**	**0.037**						
11-pp HO 4.4		**0.41**	**0.018**	**1.03**	**0.028**	**8.1**	**fixed**			**5.29/5**	**1.06**
12-AuAu0020 HO4.4		**0.815**	**0.16**	**0.49**	**0.042**	**8.1**	**fixed**			**6.6/5**	**1.32**
		0.86	0.22	0.44	0.1	8.1	fixed	0.03	0.05	6.4/4	1.60
Suppression		**1.988**	**0.400**	**0.476**	**0.043**						
HO/ H+S ratio pp		**0.619**	**0.018**	**1.114**	**0.022**						
13-pp H+S 5.9		**0.83**	**0.02**	**0.844**	**0.013**	**8.1**	**fixed**			**4.10/5**	**0.82**
HO/ H+S ratio AuAu		**0.367**	**0.086**	**1.010**	**0.133**						
14-AuAu0020H+S 5.9		**1.89**	**0.3**	**0.496**	**0.044**	**8.1**	**fixed**			**1.7/5**	**0.34**
		1.84	0.33	0.44	0.15	8.1	fixed	0.16	0.36	1.6/4	0.40
Suppression		**2.277**	**0.366**	**0.588**	**0.053**						
15-pp HO 5.9		**0.514**	**0.008**	**0.94**	**0.012**	**8.1**	**fixed**			**10.8/5**	**2.16**
16-AuAu0020 HO5.9		**0.694**	**0.12**	**0.501**	**0.049**	**8.1**	**fixed**			**9.2/5**	**1.84**
		1.33	**1.1**	**0.22**	**0.11**	**8.1**	**fixed**	**0.14**	**0.04**	**3.0/4**	**0.75**
Suppression		**1.350**	**0.234**	**0.533**	**0.053**						

FIG. 24: Results of all the fits